Crossover from fully coherent analytical approach to Maxwell Bloch equations

Stasis Chuchurka, Belarusian State University, Belarus

September 5, 2018

Abstract

The irradiation of matter by intense X-ray pulses from XFELs can result in creation of medium in which vast number of atoms is in excited state. Spontaneous emission in such system can lead to laser-like amplified spontaneous emission which was demonstrated experimentally in atomic gases [1] and solids [2]. Theoretical modeling of such systems requires accounting of quantum nature of the electromagnetic field. The quantum treatment enables correct spontaneous radiation description. However, completely quantum formalism makes the description overcomplicated and many features of radiation propagation and amplification can be described by semi-classical Maxwell-Bloch equations. A widespread approach to this problem consists of complementing the Maxwell-Bloch equations with ad-hoc noise terms mimicking the spontaneous radiation [4]. Another approach is to supply the Maxwell-Bloch equations with random initial conditions [3]. In our research group equations for correlation averages were obtained based on Heisenberg-Langevin equations. They provide us with correct description at every regime of spontaneous emission. The only problem is in enormous amount of time needed to perform numerical calculations. This contribution contains the technique that helps overcome this problem. At the very beginning of spontaneous emission one uses exact equations for correlation averages. When reached the regime where quantum effects are negligible one performs crossover to Maxwell-Bloch equations. Analytical research was made and the code was written. The comparison between the exact calculation and the simplified one is presented.

Contents

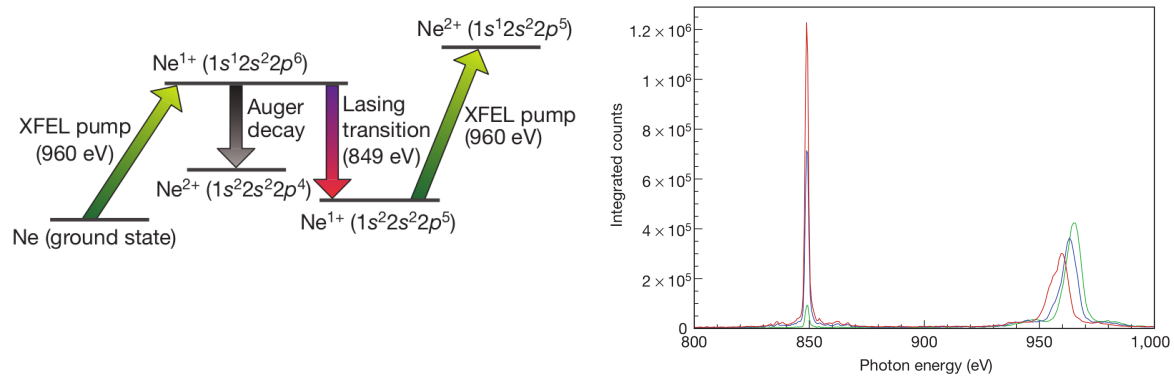

Figure 1: Taken from [1]. The first figure demonstrates the level scheme. The second figure contains single-shot spectra of the atomic x-ray laser line and transmitted XFEL pump.

1. Introduction

In 2012 atomic inner-shell X-ray laser scheme was demonstrated [1]. They observed strong amplified spontaneous emission from the end of the photo-ionized plasma (fig. 1). Obtained radiation is localized in a small solid angle and possesses high monochromaticity and wavelength stability. It means that this phenomenon can be used in studies of different subtle effects. In [6] it was shown that stimulated emission spectra contain a lot of information about substance structure. To describe spontaneous radiation correctly quantum treatment is necessary. It leads to overcomplicated formalism and many features can be described using complemented Maxwell-Bloch equations. However, all this simplified methods do not take into account non-linear quantum effects from the very initial regime properly or it is impossible to introduce pump. Usually it is pure phenomenology.

Consider some volume that is filled with atoms. Pump performs photo-ionization that leads to population inversion. Evolution of such system can be fully described with Heisenberg-Langevin equations. After quantum averaging they provide us with the information about correlation functions of atoms and field, state populations. Three approximations were used to obtain the final equations: atoms have only two levels; a correlation function of third order is replaced with correlation functions of lower orders and one-dimensional system is considered. These equations can be separated into two groups: for atomic observables and field.

For atoms we have

$$\frac{\partial \rho_{ee}(z,\tau)}{\partial \tau} = -\left(\Gamma_{sp} + \Gamma_{dec.e} + \Gamma_{nonrad}\right)\rho_{ee}(z,\tau) + p(z,\tau) - \frac{3\Delta o}{8\pi}\Gamma_{sp} n \int_0^z dz' S(z,z',\tau), \tag{1}$$

$$\frac{\partial \rho_{gg}(z,\tau)}{\partial \tau} = \left(\Gamma_{sp} + \Gamma_{nonrad}\right)\rho_{ee}(z,\tau) - \Gamma_{dec.g}\rho_{gg}(z,\tau) + \frac{3\Delta o}{8\pi}\Gamma_{sp} n \int_0^z dz' S(z,z',\tau), \quad (2)$$

$$\sigma(z,\tau) = \frac{1}{2}\left(\rho_{ee}(z,\tau) - \rho_{gg}(z,\tau)\right), \quad (3)$$

$$\frac{\partial S\left(z_1,z_2,\tau\right)}{\partial \tau} = -\Gamma_{tot} S\left(z_1,z_2\tau\right) + \frac{3\Delta o}{8\pi}\Gamma_{sp} n\left(\sigma(z_1,\tau)\int_0^{z_1} dz_1' S(z_1',z_2,\tau) + h.c\right) + \\ + \frac{3\Delta o}{8\pi}\Gamma_{sp}\left(\sigma(z_1,\tau)\rho_{ee}(z_2,\tau)H(z_1-z_2) + h.c\right), \quad (4)$$

here $\tau = t - z/c$, $\rho_{ee}(z,\tau)$ is excited state population and $\rho_{gg}(z,\tau)$ — ground state population, $\sigma(z,\tau)$ is population inversion, $S\left(z_1,z_2,\tau\right)$ is atomic correlation function, Γ_{sp} describes spontaneous decay, other Γ describe decoherence, Δo is a solid angle in which radiation mainly travels, n is a linear concentration, $p(z,\tau)$ performs pumping.

And for field

$$\frac{\partial K\left(z,\tau_1,\tau_2\right)}{\partial z} = \frac{3\Delta o}{8\pi}\Gamma_{sp} n\left(\int_0^{\tau_1} d\tau_1' \sigma\left(z,\tau_1'\right) K\left(z,\tau_1',\tau_2\right) e^{-\Gamma/2\left(\tau_1-\tau_1'\right)} + h.c\right) + \\ + \frac{3\Delta o}{64\pi\lambda^2}\Gamma_{sp} n \int_0^{Min(\tau_1,\tau_2)} d\tau' e^{-\frac{\Gamma}{2}(\tau_1+\tau_2-2\tau')}\left(\left(\Gamma_{dec.g} + \Gamma_{decoh}\right)\rho_{ee}(z,\tau') + p(z,\tau')\right), \quad (5)$$

here $K\left(z,\tau_1,\tau_2\right)$ — field correlation function and λ is a wavelength of the atomic transition.

To describe n-level system similar equations are used. The only difference: Γ should be substituted with matrices where different elements are related to different transitions.

Hereandafter the set of equations (1-5) is called the set of exact equations. The main problem of these equations is enormous amount of time spent for calculating integrals and correlation functions. The main task is to propose the algorithm capable of doing fast calculations with relatively small loss of accuracy.

The second section is dedicated to the description of the main idea. In the third section analytical results are demonstrated. The forth section contains numerical calculations and comparison between the exact calculations and the simplified ones. And the fifth section is mainly about n-level systems.

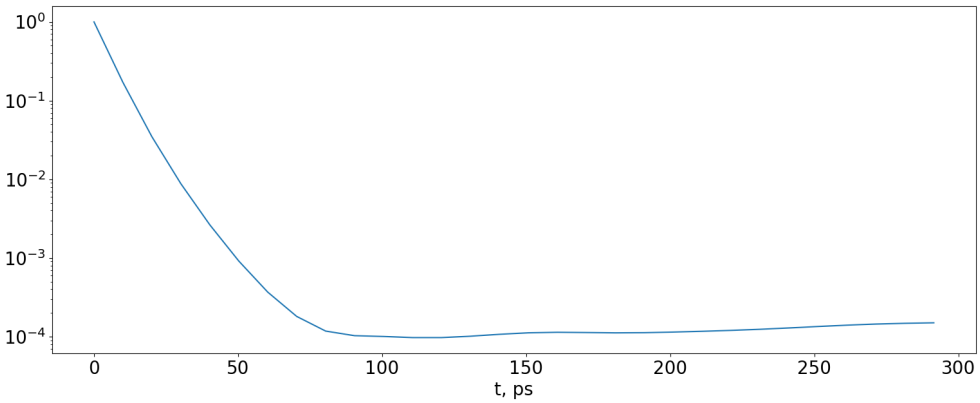

Figure 2: Numerical calculations of the quantum part contribution to the whole equation in case of atomic correlation function. One can see rapid attenuation at the beginning. At certain moment of time quantum part becomes negligible. Xenon. Total number of atoms $3 \cdot 10^5$.

2. Main idea

To make calculations faster we split the evolution of the system into two qualitatively different stages: "quantum" and "classical". Each stage is ruled by different equations: "quantum" — by the exact equations and "classical" — by the simplified ones.

2.1. Quantum regime

The first stage is mainly ruled by terms that describe spontaneous emission ("quantum parts" of equations):

$$\left(\frac{\partial S\left(z_1, z_2, \tau\right)}{\partial \tau}\right)_q = \frac{3\Delta o}{8\pi}\Gamma_{sp}\sigma(z_1,\tau)\rho_{ee}(z_2,\tau)H(z_1-z_2) + h.c., \tag{6}$$

$$\left(\frac{\partial K\left(z, \tau_1, \tau_2\right)}{\partial z}\right)_q = \frac{3\Delta o}{64\pi\lambda^2}\Gamma_{sp} n \int_0^{Min(\tau_1,\tau_2)} d\tau' e^{-\frac{\Gamma}{2}(\tau_1+\tau_2-2\tau')}\big(p(z,\tau')+$$
$$+\left(\Gamma_{dec.g}+\Gamma_{decoh}\right)\rho_{ee}(z,\tau')\big). \tag{7}$$

These terms are expected to become negligible by the end of the process. It can be seen in fig. 2.1. After the end of the quantum regime, the classical regime starts.

2.2. Classical regime

Now the quantum terms can be omitted and one obtains the following equations for the atomic variables:

$$\frac{\partial S\left(z_1,z_2,\tau\right)}{\partial\tau}=-\Gamma_{tot}S\left(z_1,z_2\tau\right)+\frac{3\Delta o}{8\pi}\Gamma_{sp}n\left(\sigma(z_1,\tau)\int_0^{z_1}dz_1'S(z_1',z_2,\tau)+h.c.\right),$$

and for the field correlation function:

$$\frac{\partial K\left(z,\tau_1,\tau_2\right)}{\partial z}=\frac{3\Delta o}{8\pi}\Gamma_{sp}n\left(\int_0^{\tau_1}d\tau_1'\sigma\left(z,\tau_1'\right)K\left(z,\tau_1',\tau_2\right)e^{-\Gamma/2\left(\tau_1-\tau_1'\right)}+h.c.\right).$$

Obtained equations result in correct observables only after entering "classical" area. Using exact equations one can obtain boundary conditions for this area.

After entering "classical" area we expect classical behaviour of correlation functions. That means we can use the following substitution:

$$S(z_1,z_2,\tau)=P(\tau,z_1)P(\tau,z_2),\quad K(z,\tau_1,\tau_2)=A(z,\tau_1)A(z,\tau_2). \tag{8}$$

In case of n-level atoms it turns out to be impossible to describe correlation function using only one term. In such case we should use a combination of classical terms (see section 5).

Performed substitution (5) one finally obtains Maxwell-Bloch equations working in classical regime:

$$\frac{\partial P\left(z,\tau\right)}{\partial\tau}=-\frac{\Gamma_{tot}}{2}P\left(z,\tau\right)+\lambda\sqrt{\frac{3\Delta o}{\pi}\Gamma_{sp}}\sigma\left(z,\tau\right)A\left(z,\tau\right), \tag{9}$$

$$\frac{A\left(z,\tau\right)}{\partial z}=\frac{n}{\lambda}\sqrt{\frac{3\Delta o}{64\pi}\Gamma_{sp}}P\left(z,\tau\right).$$

It remains to determine boundary conditions. It turns out that we should use different boundary conditions to obtain correct field and atomic correlation functions. In case of atomic observables we have to use the exact equations until certain moment of time τ_0 when quantum part is negligible. Using obtained correlation function one can determine polarization function according to (5):

$$S(z_1,z_2,\tau_0)\to P(z,\tau_0),\quad A(0,\tau)=0. \tag{10}$$

In case of field we have to use the exact equations until certain coordinate z_0 where the quantum part is negligible. Then we can use Maxwell Bloch equations with the fallowing boundary conditions:

$$K(z_0,\tau_1,\tau_2)\to A(z_0,\tau),\quad P(z,0)=0. \tag{11}$$

One can notice that the calculation of polarization results in extra calculations of field. The same thing is present in case of field, where we have additional polarization. It will be shown, that this extra field can be used to determine real field in far region. Hence, in some cases we can use the exact equations for the atomic variables only. That increases the speed of calculations significantly.

2.3. Algorithm

Finally, the code performs the following steps:

1. Calculation of atomic correlation function, excited and ground state populations using the exact equations. Each step it checks if the quantum part is small enough to make crossover to Maxwell Bloch equations.

2. When the threshold is reached the program calculates boundary conditions for polarization. Considering the correlation function as a matrix it is possible to obtain eigenvalues and eigenvectors. The eigenvector with largest contribution is used as a boundary condition for Maxwell Bloch equations.

3. Calculation of polarization, excited and ground state populations using simplified equations. During calculation the program determines pseudo field that correctly describes real field in far region.

4. Calculation of the field correlation function. Each step it checks if the quantum part is small enough to make crossover to Maxwell Bloch equations.

5. Crossover to Maxwell Bloch equations and calculation of field in line with atomic observables.

3. Analytical results for 2-level system

In approximation of a constant full population inversion it is possible to determine the atomic correlation function. It allows to obtain the analytical expression for the quantum part contribution. Hence, we can estimate the time needed to perform exact calculations.

3.1. Atomic observables for the very initial regime

Let us consider equations for the very initial case:

$$\frac{\partial S\left(z_1, z_2, \tau\right)}{\partial \tau} = \frac{3\Delta o}{16\pi}\Gamma_{sp}\left(F(z_1, z_2, \tau) + F(z_2, z_1, \tau)\right) + \frac{3\Delta o}{16\pi}\Gamma_{sp}, \tag{12}$$

$$F(z_1, z_2, \tau) = n\int_0^{z_1} dz_1' S(z_1', z_2, \tau).$$

Here we neglected pumping and term $-\Gamma_{tot}S(z_1, z_2, \tau)$. Only the terms that play significant role are left. We consider full population inversion at the beginning. To obtain the exact solution for these equations we use iterative method (Appendix A). Here we adopted the technique that is used in analyses of Takagi's equations from dynamical theory of x-ray diffraction [5]. The resulting expression for the atomic correlation function:

$$\begin{aligned} S(z_1, z_2, \tau) = \sqrt{\frac{3\Delta o\Gamma_{sp}\tau}{16\pi n}}(z_1 - z_2)^{-1}\times \\ \times\left[\sqrt{z_1}I_1\left(\sqrt{\frac{3\Delta o}{4\pi}\Gamma_{sp}\tau n z_1}\right)I_0\left(\sqrt{\frac{3\Delta o}{4\pi}\Gamma_{sp}\tau n z_2}\right) - \right. \\ \left. - \sqrt{z_2}I_1\left(\sqrt{\frac{3\Delta o}{4\pi}\Gamma_{sp}\tau n z_2}\right)I_0\left(\sqrt{\frac{3\Delta o}{4\pi}\Gamma_{sp}\tau n z_1}\right)\right]. \end{aligned} \tag{13}$$

Let us estimate population inversion change. First of all we write the simplified equation for the initial regime:

$$\frac{\partial\sigma(\tau, z)}{\partial\tau} = -\frac{3\Delta o}{8\pi}\Gamma_{sp}n\int_0^z dz' S(z, z', \tau). \tag{14}$$

Using (13) one can obtain the expression for the change of population inversion (Appendix B):

$$\begin{aligned} \Delta\sigma(\tau, z) = -\frac{3\Delta o}{16\pi}\Gamma_{sp}\int_0^\tau d\tau'\left(I_0^2\left(\sqrt{\frac{3\Delta o}{4\pi}\Gamma_{sp}\tau' n z}\right) - 1\right) = \\ = \frac{3\Delta o}{16\pi}\Gamma_{sp}\tau\left(1 + I_1^2\left(\sqrt{\frac{3\Delta o}{4\pi}\Gamma_{sp}\tau n z}\right) - I_0^2\left(\sqrt{\frac{3\Delta o}{4\pi}\Gamma_{sp}\tau n z}\right)\right). \end{aligned} \tag{15}$$

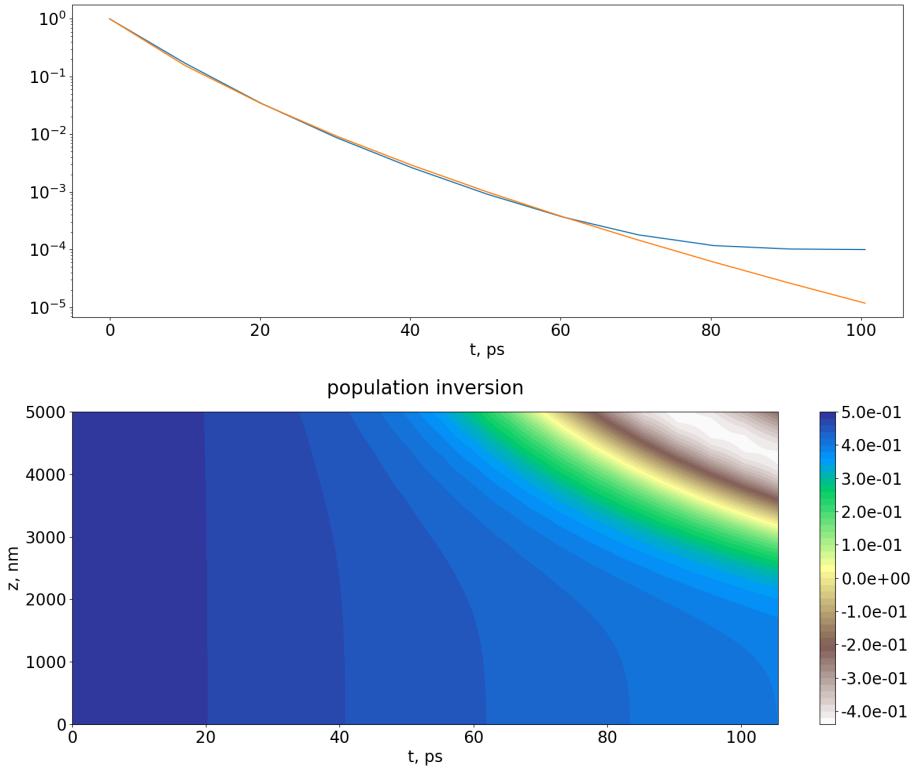

Figure 3: The first graph contains theoretical (orange line) and numerical (blue line) estimation of the quantum part contribution. The second graph shows the population inversion dependency on coordinates and time calculated numerically. Xenon. Total number of atoms $3 \cdot 10^5$.

3.2. Estimation of quantum term contribution. Analytical expression for classical regime boundary conditions

Since we are mainly interested in time dependency, one can average over coordinates the expression for the atomic correlation function:

$$S(\tau) = \frac{1}{L^2} \int S(z_1, z_2, \tau) dz_1 dz_2,$$

here L is size of the system.

To estimate quantum part contribution we divide the second term from right hand side of equation by $dS(\tau)/d\tau$. Using the result of the previous subsection one obtains the following expression (Appendix C):

$$\varepsilon(\tau) = \frac{\frac{3\Delta o}{16\pi}\Gamma_{sp}}{dS(\tau)/d\tau} = \frac{\frac{3\Delta o}{16\pi}\Gamma_{sp} N\tau}{I_1^2\left(\sqrt{\frac{3\Delta o}{4\pi}\Gamma_{sp} N\tau}\right)}, \tag{16}$$

here N is a total number of atoms. Fig. 3 contains comparison between theory and simulation. Using function $\varepsilon(\tau)$ it is simple to determine the time needed to finish the

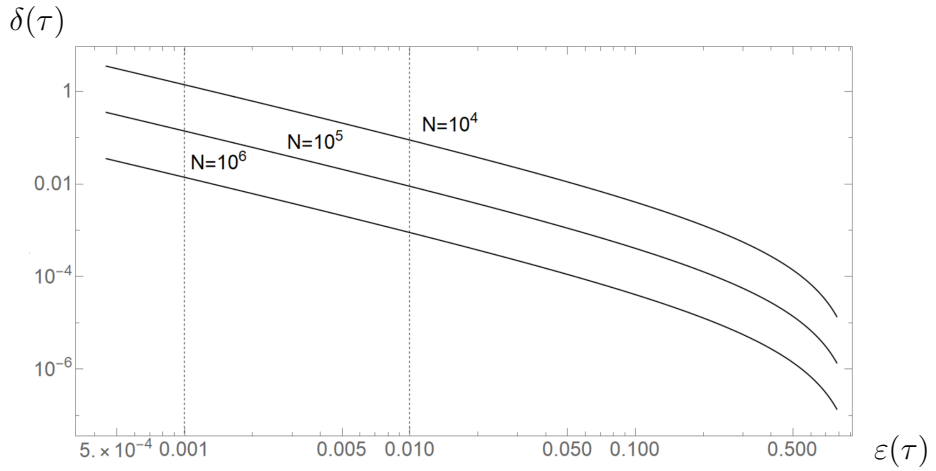

Figure 4: Relation between $\delta(\tau)$ and $\varepsilon(\tau)$ for different number of atoms N.

quantum regime. In order to take pumping into account one should estimate pumping time and subtract it from τ.

All expressions in this chapter are derived within approximation $\sigma = 1/2$. To estimate an error connected with this approximation let us average $\Delta\sigma$ over coordinates and multiply by two:

$$\delta(\tau) = \frac{3\Delta o}{8\pi}\Gamma_{sp}\tau\left[1 + 2I_1^2\left(\sqrt{\frac{3\Delta o}{4\pi}\Gamma_{sp}\tau N}\right) - I_0\left(\sqrt{\frac{3\Delta o}{4\pi}\Gamma_{sp}\tau N}\right)\times\right.$$
$$\left.\times\left(I_0\left(\sqrt{\frac{3\Delta o}{4\pi}\Gamma_{sp}\tau N}\right) + I_2\left(\sqrt{\frac{3\Delta o}{4\pi}\Gamma_{sp}\tau N}\right)\right)\right]. \quad (17)$$

This function shows the deviation of the population inversion from 1/2. It should be small enough to use formula (16). Fig. 4 shows the relation between $\delta(\tau)$ and $\varepsilon(\tau)$.

If accuracy is acceptable and the quantum part is small enough one can use (13) to obtain boundary condition for classical regime. In case of $\frac{z}{L} \gg \left(\frac{3\Delta o}{4\pi}\Gamma_{sp}\tau_0 N\right)^{-1}$:

$$P(\tau_0, z) \approx \left(\frac{3\Delta o\Gamma_{sp}\tau_0}{64\pi nz}\right)^{1/4} I_0\left(\sqrt{\frac{3\Delta o}{4\pi}\Gamma_{sp}\tau_0 nz}\right), \quad \Delta\sigma(\tau_0, z) \approx -P(\tau_0, z). \quad (18)$$

It is interesting to compare (18) with the technique used in [3] based on random initial conditions. The result can be rewritten in the following way:

$$P(\tau_0, z) = \sqrt{\frac{L}{Nz}} f\left(\frac{3\Delta o}{4\pi}\Gamma_{sp}\tau_0 nz\right),$$

here f is a function that depends on the moment of the transition to classical regime. Range of $\sqrt{\frac{L}{Nz}}$ is $N^{-1/2}$. In [3] we have random initial conditions with range of $N^{-1/2}$ as well. However, our treatment provides us with correct description at the beginning of the process and does not need considering statistical ensemble.

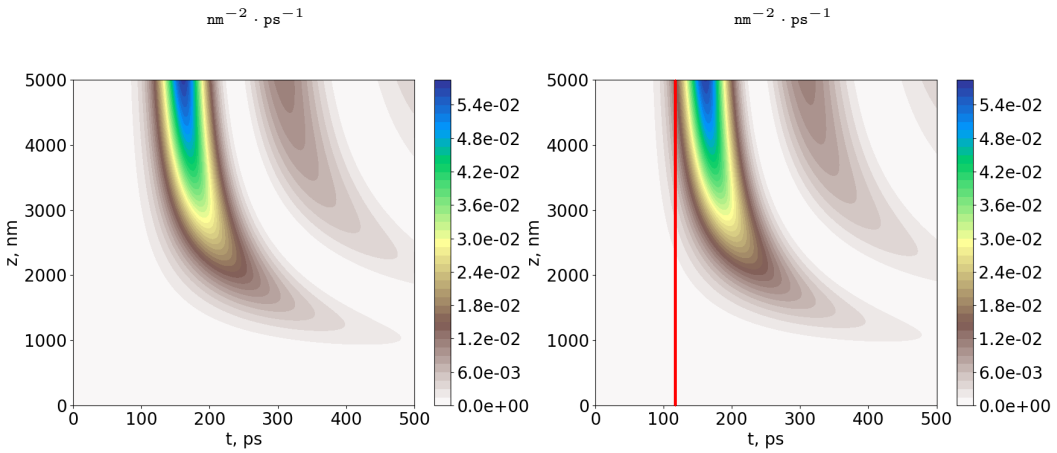

Figure 5: The first graph contains the intensity of radiation calculated with exact equations, the second graph — with simplified ones. Red line shows the time of transition to the classical regime.

4. Numerical results for 2-level system

In this section we demonstrate numerical results, comparison between exact calculations and simplified ones for 2-level system.

In simulations we considered Xenon with $\Gamma_{sp}^{-1} = 1.0$ ns, $L = 5.0 \cdot 10^3$ nm, $N = 3 \cdot 10^5$, $\lambda = 65$ nm, $\Delta o = 0.013$. Table 1 contains the information about the time needed to perform simulations on my laptop.

Table 1: Time needed to perform simulations

Equations	quantum regime	classical regime	total
Exact for atomic observables	1 min 50 sec	—	1 min 50 sec
Simplified for atomic observables	19 sec	1 sec	20 sec
Exact for field	1 min 15 sec	—	1 min 15 sec
Simplified for field	13 sec	1 sec	14 sec

One can see that proposed algorithm works much faster with almost no loss in accuracy. That is the case for the intensity (number of photons per cross section per solid angle per a unit of time) of radiation (fig. 5), state populations (fig. 6 – 7) and atomic correlation functions (fig. 9).

In case of field correlation functions we have more things to discuss (fig. 10). First of all one can see noticeable difference between correlation functions obtained with exact and simplified equations for large distances (fig. 8). Even if the average quantum part is small, that is not the case for each point separately. Ideally we should divide the time into small intervals and check the quantum part and perform the transition individually for each region. The second peculiar thing is that pseudo field (see 2.3) results in correct correlation function for large distances. In other words the pseudo field coincides with the real field in far region.

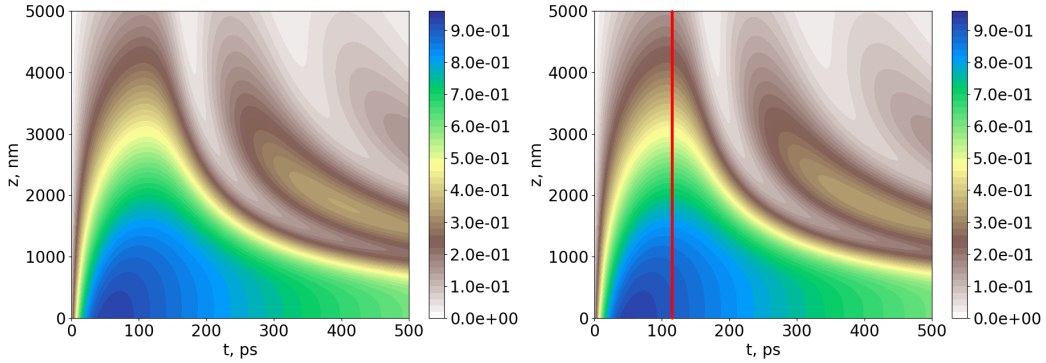

Figure 6: The first graph contains the ground state population calculated with exact equations, the second graph — with simplified ones.

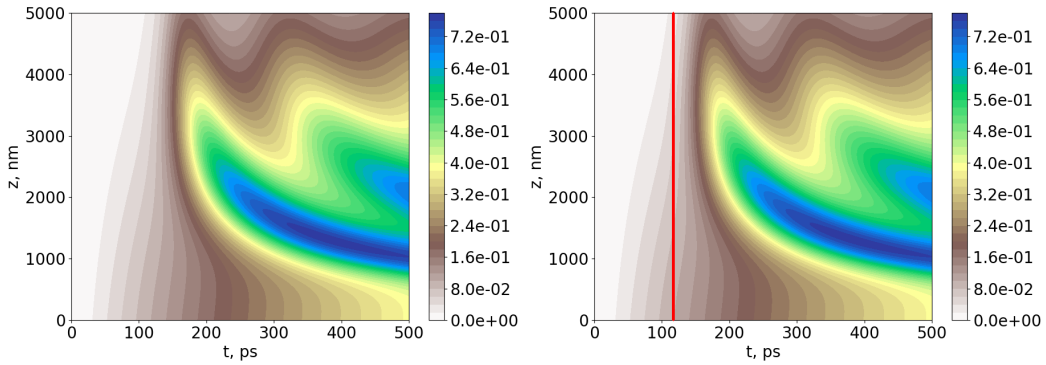

Figure 7: Similarly for the excited state population.

$$K(z,\tau,\tau)\ \ \mathtt{nm}^{-2}\cdot\mathtt{ps}^{-1}$$

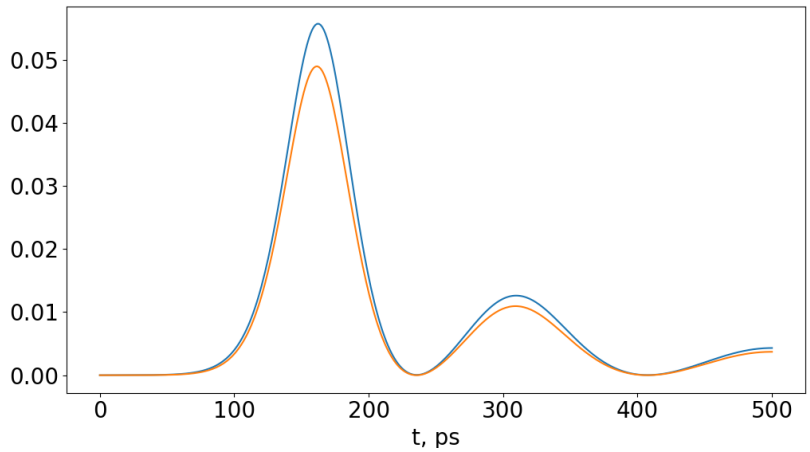

Figure 8: Intensity at the end of the system. Blue line — exact method, orange line — simplified one.

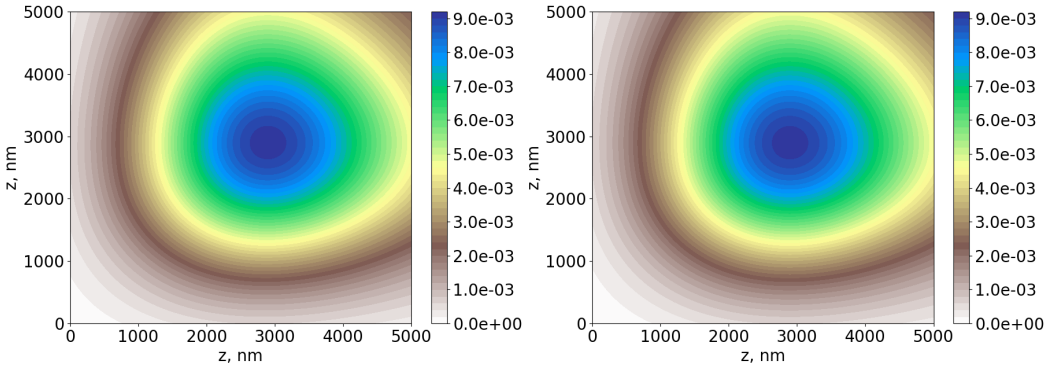

$\tau = 120$ ps

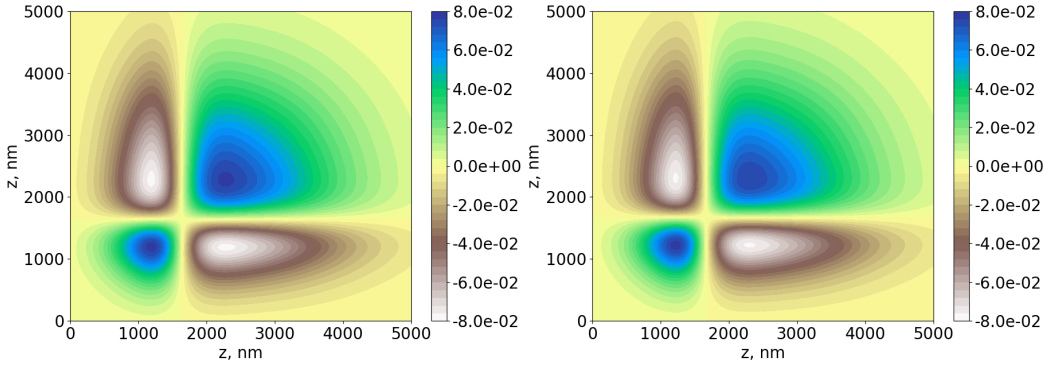

$\tau = 310$ ps

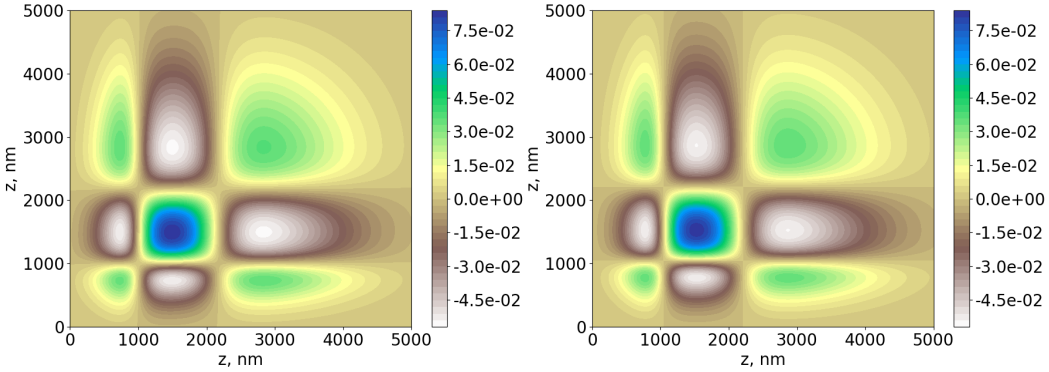

$\tau = 500$ ps

Figure 9: The first column contains exact simulations for atomic correlation function of different moments of time, the second — simplified simulations.

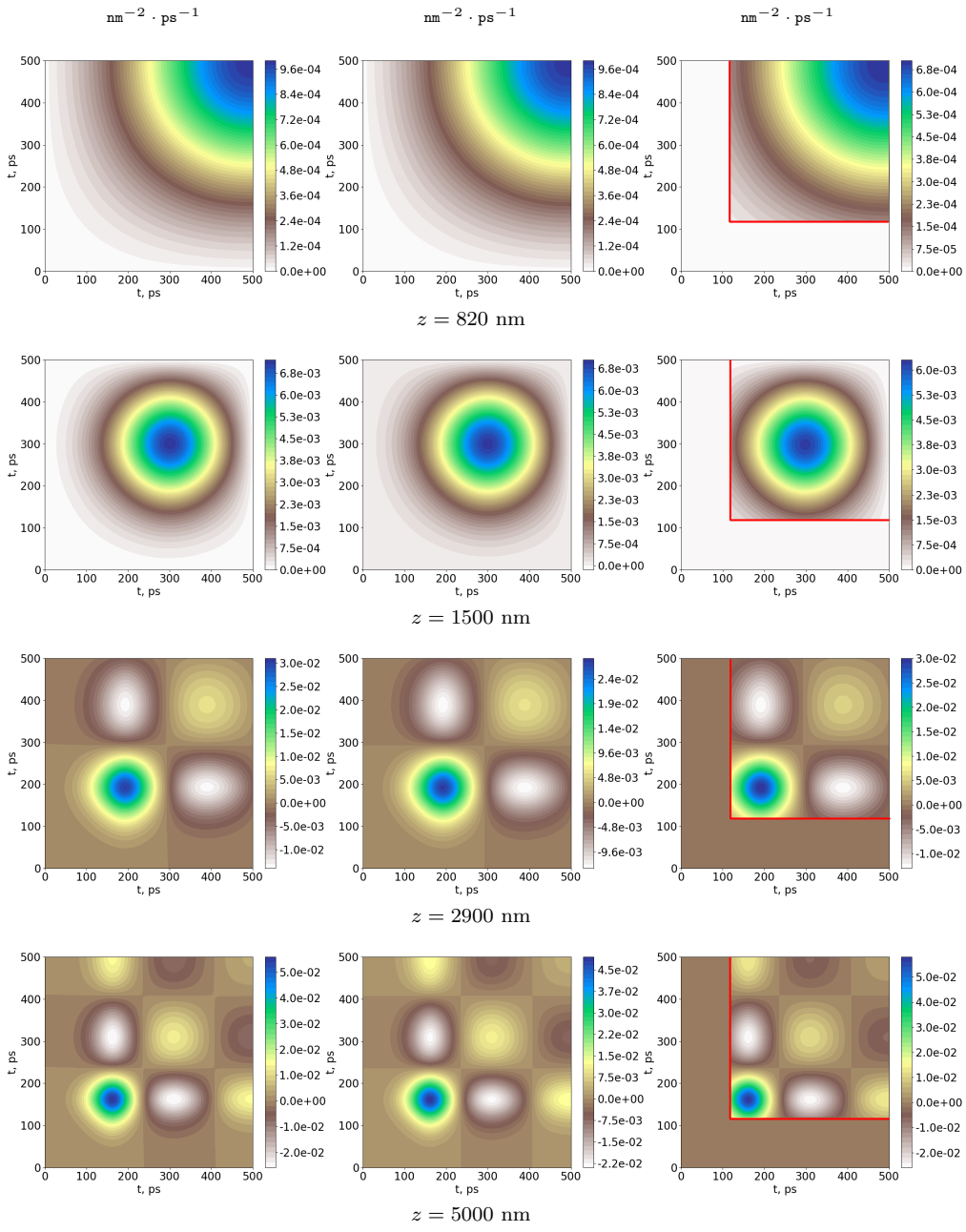

Figure 10: The first column contains exact simulations for atomic correlation function of different coordinates, the second — simplified simulations, the third column contains correlation functions built out of pseudo field functions. Red line shows the time of transition to classical regime.

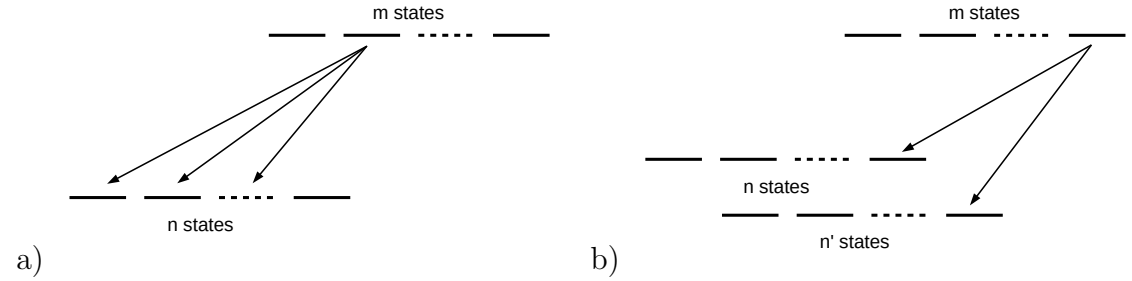

Figure 11: a) 2-level scheme with degenerate states; b) Λ scheme with degenerate states.

5. n-level systems

In this section we consider different n-level schemes: $1s_{1/2} \to 2p_{1/2}$, Λ level scheme with different ground state energies and $1s_{1/2} \to 2p_{1/2}, 2p_{3/2}$. All results are obtained for the case of incoherent pumping. Equations for n-level system turn to be too bulky to mention them here.

Accounting for different transitions leads to impossibility of the "classical" expansion. Now we use the following expression:

$$S_{p,q}(z_1, z_2, \tau) = \sum_i P^*_{p,i}(\tau, z_1) P_{q,i}(\tau, z_2),$$

here p and q denote atomic transitions. The number of terms depends on the accuracy you need (usually we use 2 terms and accuracy was satisfying). From now we should add the following step to the algorithm: when obtaining boundary conditions for classical regime the program picks a set of eigenvectors. The number of eigenvectors depends on the accuracy required.

5.1. $1s_{1/2} \to 2p_{1/2}$ level scheme. 2-level systems with degenerate states

Here, 2 degenerate ground states and 2 degenerate excited states are presented. It turns out that such type of systems can be substituted with 2-level one with no loss in accuracy due to the fact that we can flip the system and nothing would change. In terms of speed we have the same result for the simplified algorithm as it was in case of a 2-level system. Exact atomic equations for the full $1s_{1/2} \to 2p_{1/2}$ level scheme costs approximately $(2 \cdot 2)^2 = 16$ times more (24 min against 20 sec). $2 \cdot 2$ is for all possible transitions and the second power — for correlation function depending on 2 transitions.

The same simplification can be performed for any type of system composed of 2 energy levels (fig. 11a). Hence, in case of n degenerate ground states and m degenerate excited states we can reduce the system to n/2 and m/2 states respectively.

In case of incoherent pumping, only diagonal elements of state populations turn non-zero. That is used to make the code even faster.

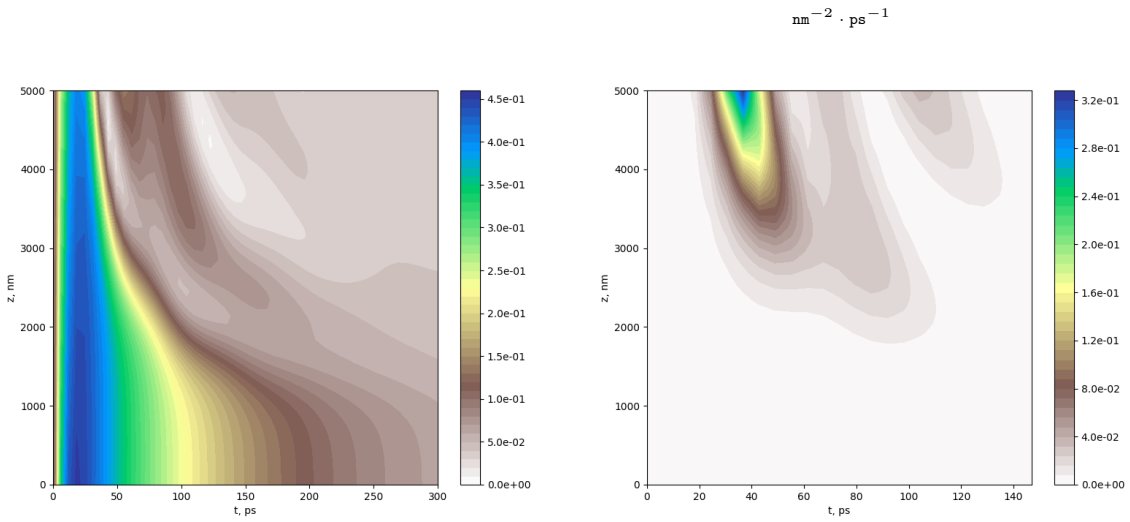

Figure 12: Excited state population for one of degenerate states and resulting intensity.

5.2. Λ system with different ground state energies. Numerical example for $1s_{1/2} \to 2p_{1/2}, 2p_{3/2}$

The main property of Λ system (fig. 11b) is that some non-diagonal elements become non-zero as well as diagonal. It turns out that they related to the levels of the same total angular momentum projection.

As in previous subsection it is possible to reduce such type of system to twice smaller one as well.

In fig. 12 – 13 one can see the result of program work. $1s_{1/2} \to 2p_{1/2}, 2p_{3/2}$ is considered. Threshold time — 30 ps.

6. Conclusion

We have presented the formalism that describes amplified spontaneous emission in one dimensional system properly. Since it needs a lot of resources to be simulated, we have demonstrated a technique that optimizes it. The comparison between exact and optimized approaches has been presented. The code for 2-level and n-level systems is written.

$1s_{1/2} \to 2p_{1/2}\ (\Delta m = 1),\ \ 1s_{1/2} \to 2p_{1/2}\ (\Delta m = 1)$

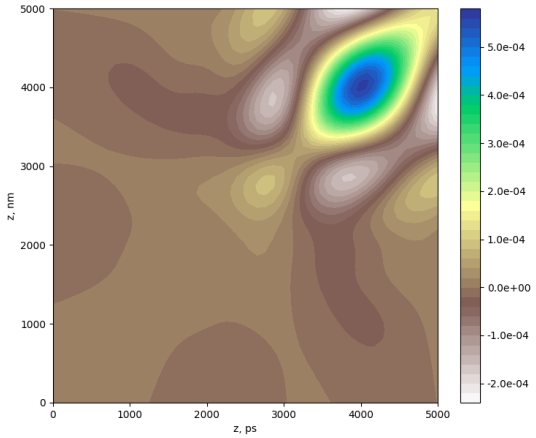

$1s_{1/2} \to 2p_{1/2}\ (\Delta m = 1),\ \ 1s_{1/2} \to 2p_{3/2}\ (\Delta m = 1)$

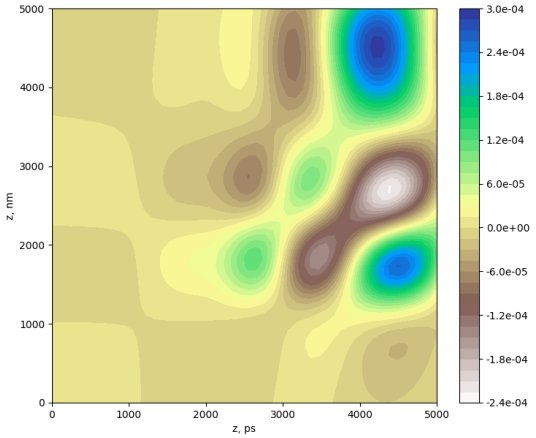

$1s_{1/2} \to 2p_{1/2}\ (\Delta m = 1),\ \ 1s_{1/2} \to 2p_{3/2}\ (\Delta m = -1)$

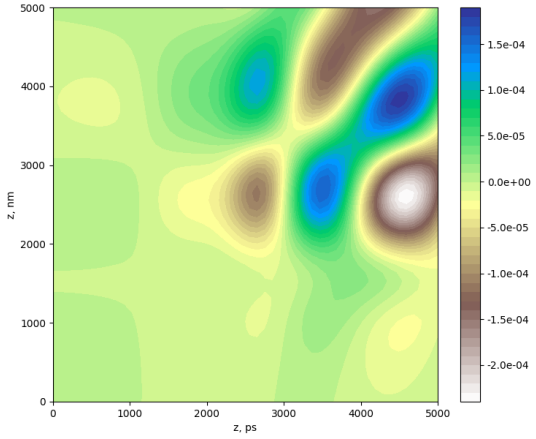

$1s_{1/2} \to 2p_{3/2}\ (\Delta m = 1),\ \ 1s_{1/2} \to 2p_{3/2}\ (\Delta m = 1)$

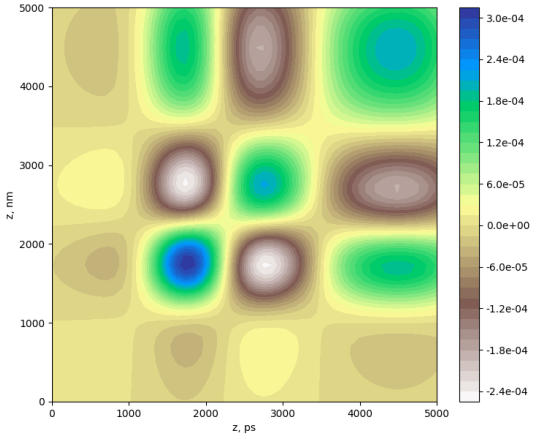

$1s_{1/2} \to 2p_{1/2}\ (\Delta m = -1),\ \ 1s_{1/2} \to 2p_{3/2}\ (\Delta m = 1)$

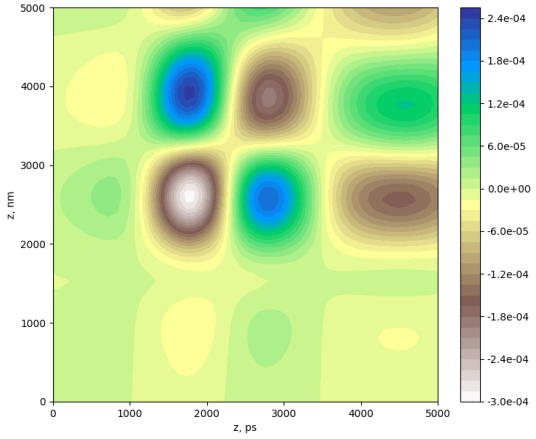

$1s_{1/2} \to 2p_{3/2}\ (\Delta m = -1),\ \ 1s_{1/2} \to 2p_{3/2}\ (\Delta m = -1)$

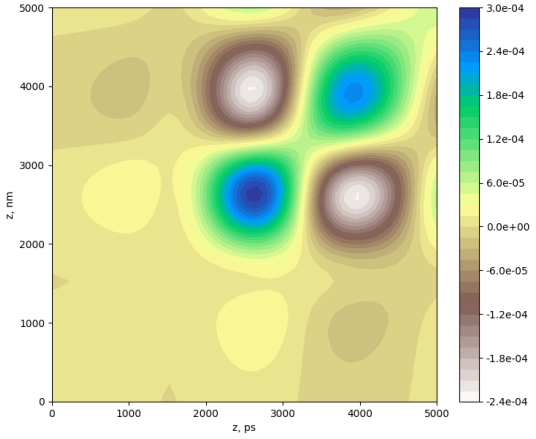

Figure 13: Correlation functions for different transitions at $\tau = 300$ fs. Consider only positive momentum projections.

Appendix A Derivation of atomic correlation function

To obtain the exact solution for (12) we use iterative method:

$$S_0(z_1,z_2,\tau)=0,\quad F_0(z_1,z_2,\tau)=0, \tag{19}$$

$$S_1(z_1,z_2,\tau)=\frac{3\Delta o}{16\pi}\Gamma_{sp}\tau,\quad F_1(z_1,z_2,\tau)=\frac{3\Delta o}{16\pi}\Gamma_{sp}\tau n z_1,$$

$$S_2(z_1,z_2,\tau)=\frac{3\Delta o}{16\pi}\Gamma_{sp}\tau+\frac{1}{2}\left(\frac{3\Delta o}{16\pi}\Gamma_{sp}\tau\right)^2 n(z_1+z_2),$$

$$S_i(z_1,z_2,\tau)=\frac{3\Delta o}{16\pi}\Gamma_{sp}\tau+...+\frac{1}{i!}\left(\frac{3\Delta o}{16\pi}\Gamma_{sp}\tau\right)^i f_{i-1}(z_1,z_2),$$

$$f_i(z_1,z_2)=\frac{n^i}{i!}\sum_{j=0}^{i}\binom{i}{j}^2 z_1^j z_2^{i-j}.$$

This iterative process results in

$$S(z_1,z_2,\tau)=\sum_{i=0}^{\infty}\frac{1}{(i+1)!}\left(\frac{3\Delta o}{16\pi}\Gamma_{sp}\tau\right)^{i+1} f_i(z_1,z_2).$$

Changing the order of summation

$$S(z_1,z_2,\tau)=\sum_{j=0}^{\infty}\frac{(nz_1)^j}{j!^2}\sum_{i=j}^{\infty}\frac{\left(\frac{3\Delta o}{16\pi}\Gamma_{sp}\tau\right)^{i+1}(nz_2)^{i-j}}{(i+1)(i-j)!^2}$$

transforms resulting expression to the integral over time and shifts the index in the second sum:

$$S(z_1,z_2,\tau)=\int_0^{\frac{3\Delta o}{16\pi}\Gamma_{sp}\tau}\sum_{j=0}^{\infty}\frac{(xnz_1)^j}{j!^2}\sum_{i=0}^{\infty}\frac{(xnz_2)^i}{i!^2}dx. \tag{20}$$

Each sum turns out to be a representation of Bessel function:

$$S(z_1,z_2,\tau)=\int_0^{\frac{3\Delta o}{16\pi}\Gamma_{sp}\tau} I_0\left(2\sqrt{xnz_1}\right) I_0\left(2\sqrt{xnz_2}\right) dx.$$

It is appropriate to rewrite the integral

$$S(z_1,z_2,\tau)=\frac{1}{2}\int_0^{\sqrt{\frac{3\Delta o}{4\pi}\Gamma_{sp}\tau}} xI_0\left(x\sqrt{nz_1}\right) I_0\left(x\sqrt{nz_2}\right) dx$$

to use properties of Bessel function:

$$\begin{aligned}S(z_1,z_2,\tau)=\sqrt{\frac{3\Delta o\Gamma_{sp}\tau}{16\pi n}}(z_1-z_2)^{-1}\times\\ \times\left[\sqrt{z_1}I_1\left(\sqrt{\frac{3\Delta o}{4\pi}\Gamma_{sp}\tau n z_1}\right)I_0\left(\sqrt{\frac{3\Delta o}{4\pi}\Gamma_{sp}\tau n z_2}\right)-\right.\\ \left.-\sqrt{z_2}I_1\left(\sqrt{\frac{3\Delta o}{4\pi}\Gamma_{sp}\tau n z_2}\right)I_0\left(\sqrt{\frac{3\Delta o}{4\pi}\Gamma_{sp}\tau n z_1}\right)\right].\end{aligned} \tag{21}$$

Appendix B Derivation of population inversion change

To obtain right hand side of the equation we use (20):

$$n\int_0^z dz' S(z,z',\tau) = \int_0^{\frac{3\Delta o}{16\pi}\Gamma_{sp}\tau} \sum_{j=0}^{\infty} \frac{(xnz)^j}{j!^2} \sum_{i=0}^{\infty} \frac{(xnz)^{i+1}}{i!(i+1)!} \frac{dx}{x}. \tag{22}$$

As in the previous section each sum can be replaced with Bessel function:

$$n\int_0^z dz' S(z,z',\tau) = \int_0^{\frac{3\Delta o}{16\pi}\Gamma_{sp}\tau} \sqrt{\frac{nz}{x}} I_0(2\sqrt{xnz}) I_1(2\sqrt{xnz}) dx.$$

Finally let us perform the integration:

$$n\int_0^z dz' S(z,z',\tau) = \int_0^{\sqrt{\frac{3\Delta o}{4\pi}\Gamma_{sp}\tau}} I_0(x\sqrt{nz}) I_1(x\sqrt{nz}) dx = \\ = \frac{1}{2}\left(I_0^2\left(\sqrt{\frac{3\Delta o}{4\pi}\Gamma_{sp}\tau nz}\right) - 1\right).$$

Using (14) one expresses the population inversion change:

$$\Delta\sigma(\tau,z) = -\frac{3\Delta o}{16\pi}\Gamma_{sp}\int_0^{\tau} d\tau' \left(I_0^2\left(\sqrt{\frac{3\Delta o}{4\pi}\Gamma_{sp}\tau' nz}\right) - 1\right) = \\ = \frac{3\Delta o}{16\pi}\Gamma_{sp}\tau\left(1 + I_1^2\left(\sqrt{\frac{3\Delta o}{4\pi}\Gamma_{sp}\tau nz}\right) - I_0^2\left(\sqrt{\frac{3\Delta o}{4\pi}\Gamma_{sp}\tau nz}\right)\right). \tag{23}$$

Appendix C Estimation of quantum term contribution

Let us derive the expression for the average atomic correlation function:

$$S(\tau) = \int_0^{\frac{3\Delta o}{16\pi}\Gamma_{sp}\tau} \left(\sum_{j=0}^{\infty} \frac{(xN)^j}{j!(j+1)!} \right)^2 dx, \tag{24}$$

here N is a total number of atoms. The next step is to substitute sum with Bessel function:

$$S(\tau) = \int_0^{\frac{3\Delta o}{16\pi}\Gamma_{sp}\tau} \frac{1}{xN} I_1^2\left(2\sqrt{xN}\right) dx.$$

To estimate the quantum part contribution we divide the second term from right hand side of equation (12) by $\frac{dS(\tau)}{d\tau}$:

$$\varepsilon(\tau) = \frac{\frac{3\Delta o}{16\pi}\Gamma_{sp}}{dS(\tau)/d\tau} = \frac{\frac{3\Delta o}{16\pi}\Gamma_{sp} N\tau}{I_1^2\left(\sqrt{\frac{3\Delta o}{4\pi}\Gamma_{sp} N\tau}\right)}. \tag{25}$$

References

[1] Nina Rohringer, Duncan Ryan, Richard A London, Michael Purvis, Felicie Albert, James Dunn, John D Bozek, Christoph Bostedt, Alexander Graf, Randal Hill, et al. Atomic inner-shell x-ray laser at 1.46 nanometres pumped by an x-ray free-electron laser. Nature, 481(7382):488, 2012.

[2] Hitoki Yoneda, Yuichi Inubushi, Kazunori Nagamine, Yurina Michine, Haruhiko Ohashi, Hirokatsu Yumoto, Kazuto Yamauchi, Hidekazu Mimura, Hikaru Kitamura, Tetsuo Katayama, et al. Atomic inner-shell laser at 1.5-ngstrm wavelength pumped by an x-ray free-electron laser. Nature, 524(7566):446, 2015.

[3] Michel Gross and Serge Haroche. Superradiance: An essay on the theory of collective spontaneous emission. Physics reports, 93(5):301396, 1982.

[4] O. Larroche, D. Ros, A. Klisnick, A. Sureau, C. Mller, and H. Guennou. Maxwell-bloch modeling of x-ray-laser-signal buildup in single- and double-pass configurations. Phys. Rev. A, 62:043815, Sep 2000.

[5] A. Authier. Dynamical Theory of X-Ray Diffraction. Oxford University Press. 2001

[6] Thomas Kroll, Clemens Weninger, Roberto Alonso-Mori, Dimosthenis Sokaras, Diling Zhu, Laurent Mercadier, Vinay P. Majety, Agostino Marinelli, Alberto Lutman, Marc W. Guetg, Franz-Josef Decker, Sbastien Boutet, Andy Aquila, Jason Koglin, Jake Koralek, Daniel P. DePonte, Jan Kern, Franklin D. Fuller, Ernest Pastor, Thomas Fransson, Yu Zhang, Junko Yano, Vittal K. Yachandra, Nina Rohringer, and Uwe Bergmann, et al. Stimulated X-Ray Emission Spectroscopy in Transition Metal Complexes. Phys. Rev. Let., 120:133203, Mar 2018.